Hyperbolic attractor in a system of coupled non-autonomous van der Pol oscillators: Numerical test for expanding and contracting cones

S.P. Kuznetsov and I.R. Sataev

Institute of Radio-Engineering and Electronics of RAS, Saratov Branch,
Zelenaya 38, 410019, Saratov, Russian Federation

Abstract

We present numerical verification of hyperbolic nature for chaotic attractor in a system of two coupled non-autonomous van der Pol oscillators (Kuznetsov, Phys. Rev. Lett., **95,** 144101, 2005). At certain parameter values, in the four-dimensional phase space of the Poincaré map a toroidal domain (a direct product of a circle and a three-dimensional ball) is determined, which is mapped into itself and contains the attractor we analyze. In accordance with the computations, in this absorbing domain the conditions of hyperbolicity are valid, which are formulated in terms of contracting and expanding cones in the tangent spaces (the vector spaces of the small state perturbations).

Mathematical theory of chaotic dynamics based on a rigorous axiomatic foundation exploits a concept of hyperbolicity [1-8].

An orbit in phase space of a dynamical system is called hyperbolic if there are trajectories approaching exponentially the original orbit, and those departing from it in a similar manner. Moreover, an arbitrary small perturbation of a state on the original orbit must admit representation via a linear combination of the growing and the decaying perturbations.

In dissipative systems contracting the space volume the attractors may occur, which consist exclusively of the hyperbolic orbits. These are attractors with strong chaotic properties, like existence of the well-defined invariant SRB-measure, a possibility of description in terms of Markov partitions and symbolic dynamics, positive metric and topological entropy etc. Such hyperbolic (or, more definitely, *uniformly hyperbolic*) attractors are robust or structurally stable, that means insensitivity of the type of dynamics and of the phase space structure in respect to slight variations of functions and parameters in the evolutionary equations.

Although the basic statements of the hyperbolic theory were formulated 40 years ago, no convincing examples of physical systems were introduced with uniform hyperbolic attractors. In textbooks and reviews on nonlinear dynamics, such attractors are represented by artificial mathematical constructions, like Plykin attractor and Smale – Williams solenoid [1-8]. For realistic systems, in which the chaotic dynamics is mathematically proved, like the Lorenz model [9,10], the strange attractors do not relate to

the class of uniformly hyperbolic (not all axiomatic statements of the classic hyperbolic theory are valid for them). Some aspects of possible existence of hyperbolic attractors in differential equations were discussed e.g. in Refs. [11-14].

In a recent paper of one of the authors [15], an idea was advanced of implementation of a hyperbolic attractor in a system of two coupled non-autonomous van der Pol oscillators. In a Poincaré map that determines evolution on a period of the external driving, a chaotic attractor has been found, which demonstrates some characteristic signs of hyperbolic attractors. By a nature of transformation of the phase space volume in a course of the evolution over a period, it is similar to the Smale – Williams solenoid. It looks robust: the Cantor-like transverse structure and the positive Lyapunov exponent are insensitive to variation of parameters in the equations. An analogous system has been built as an electronic device and studied in experiment [16].

Obviously, it would be desirable to have a mathematical confirmation of the hyperbolic nature of the attractor. As Sinai has suggested in due time [1], one possible way for substantiation of the hyperbolicity for attractor of a Poincaré map consists in numerical verification of certain sufficient conditions formulated in terms of inclusion for expanding and contracting cones in tangent vector space (the space of small perturbation vectors). In this paper, we discuss a method and present results of computer verification of these conditions in application to the chaotic attractor in a system of two coupled non-autonomous van der Pol oscillators.

The system proposed in Ref. [15] is represented by a set of differential equations

$$\begin{array}{ll} \dot{x} = \omega_0 u, & \dot{u} = -\omega_0 x + (A\cos 2\pi t/T - x^2)u + (\varepsilon/\omega_0) y \cos\omega_0 t, \\ \dot{y} = 2\omega_0 v, & \dot{v} = -2\omega_0 y + (-A\cos 2\pi t/T - y^2)v + (\varepsilon/2\omega_0)x^2. \end{array} \tag{1}$$

It consists of two subsystems, the van der Pol oscillators with characteristic frequencies ω_0 and $2\omega_0$. Here x and u represent coordinate and velocity for the first oscillator, and y and v for the second one. In each oscillator the parameter responsible for the birth of the limit cycle, is forced to swing slowly with period T and amplitude A. As the parameter modulation is of opposite phase, the subsystems generate turn by turn, each on its own half-period T. The coupling is characterized by parameter ε. The first oscillator affects the second one via a quadratic term in the equation. The backward coupling is introduced by a product of the variable y and an auxiliary signal of frequency ω_0. It is assumed that the interval T contains an integer number of periods of the auxiliary signal $N_0 = \omega_0 T/2\pi$, so the external driving is periodic. For a detailed study, we select

$$\omega_0 = 2\pi,\ T = 6,\ A = 5,\ \varepsilon = 0.5. \tag{2}$$

Qualitatively, the system (1) operates as follows. Let the first oscillator on a stage of generation have some phase ψ: $x \propto \sin(\omega_0 t + \psi)$. The squared value x^2 contains the second harmonic: $\cos(2\omega_0 t + 2\psi)$, and its phase is 2ψ. As the half-period comes to the end, the term x^2 effects as priming for the excitation of the second oscillator, and the oscillations of y get the phase 2ψ. Half a period later, the mixture of these oscillations with the auxiliary signal stimulates excitation of the first oscillator, which accepts this phase 2ψ. Obviously, on subsequent periods the phase of the first oscillator will follow approximately the relation

$$\psi_{n+1} = 2\psi_n + \text{const}\ \ (\text{mod}2\pi). \tag{3}$$

(Here the constant accounts a phase shift in a course of transfer of the excitation from one oscillator to another and back.) The relation (3) called the Bernoulli map is well known as one of the simplest model examples in the chaos theory.[1]

For accurate description of the discrete time dynamics, we turn to the Poincaré map [2-8, 17,18]. Let us have a vector $\mathbf{x}_n = \{x(t_n), u(t_n), y(t_n), v(t_n)\}$ as a state of the system at t_n=nT. From solution of the differential equations (1) with the initial condition $\mathbf{x}_n$, we get a new vector $\mathbf{x}_{n+1}$ at t_{n+1}=$(n+1)T$. As it is determined uniquely by $\mathbf{x}_n$, we introduce a function that maps the four-dimensional space $\{x, u, y, v\}$ into itself: $\mathbf{x}_{n+1} = \mathbf{T}(\mathbf{x}_n)$.

This Poincaré map appears due to evolution determined by differential equations with smooth and bounded right-hand parts in a finite domain of variables $\{x, u, y, v\}$. In accordance with theorems of existence, uniqueness, continuity, and differentiability of solutions of differential equations, the map $\mathbf{T}$ is a diffeomorphism, a one-to-one differentiable map of class C^∞ [17].

Further, we will deal always with description of the dynamics in terms of the Poincaré map. In particular, under the phase space we mean the four-dimensional space $\{x, u, y, v\}$, with x, u, y, v relating to an instant t_n. An orbit means a discrete sequence of points in this space; attractor is an invariant attractive set composed of such orbits etc.

In a course of iterations of the map $\mathbf{x}_{n+1} = \mathbf{T}(\mathbf{x}_n)$, we have expansion of a small phase-space volume in a direction associated with the phase in the approximate equation (3) and contraction in the rest three directions. Interpreting the mapping geometrically, let us imagine a solid toroid embedded in the 4-dimensional space (a direct product of a circle and a three-dimensional ball) and associate one iteration of the map with longitudinal stretch of the toroid, with contraction in the transversal directions, and insertion of the doubly folded "tube" into the original toroid. It is analogous to the construction of Smale and Williams with the only difference that we deal with four-dimensional rather than the three-dimensional phase space.

The mentioned toroid will be referred to as an absorbing domain U. It means that under application of the map $\mathbf{T}$ the images of all points from U belong to its interior: $\mathbf{T}(U) \subset \mathrm{Int}\, U$. The attractor may be defined as intersection of the images of the original domain under multiple action of the map: $A = \bigcap_{n=1}^{\infty} \mathbf{T}^n(U)$.

To write down an analytic expression for the domain U it is convenient to redefine the coordinate system. We introduce new variables $\{x_0, x_1, x_2, x_3\}$ as follows:

$$x_0 = x/r_0, \quad x_1 = (u - c_{ux}x)/r_1, \quad x_2 = y - c_{yx}x - c_{yu}u, \quad x_3 = v - c_{vx}x - c_{vu}u - c_{vy}y. \quad (4)$$

To determine the constants we accumulate a large number of points $\{x, u, y, v\}$ on the attractor in the Poincaré section by numerical solution of the equations (1). Then, by the least square method we find out the coefficients to minimize the mean-square values $< (u - c_{ux}x)^2 >$, $< (y - c_{yx}x - c_{yu}u)^2 >$, $< (v - c_{vx}x - c_{vu}u - c_{vy}y)^2 >$. Geometrically, it corresponds to directing the coordinate axes along the principal axes of ellipsoid that approximates the attractor. Additionally, we normalize x_0 and x_1 by appropriate factors

[1]The constant in Eq. (3) may be removed by a shift of origin for the phase variable. We stress that the phase ψ cannot be defined globally on the whole time interval T: it has sense only in the context of the discrete time description. Indeed, on the stage when the first oscillator does not generate, its amplitude is small, and phase is not well defined.

to have ¡x_0^2¿=¡x_1^2¿≈1/2. Finally, at the parameter set (2) we get

$$\begin{array}{llll} c_{ux} = 0.438, & c_{yx} = -0.042, & c_{yu} = 0.226, & c_{vx} = -0.218, \\ c_{vu} = 0.029, & c_{vy} = -0.118, & r_0 = 0.812, & r_1 = 0.721. \end{array} \tag{5}$$

In the new coordinates, let us define the absorbing domain U by the inequality:

$$\left[\left(\sqrt{x_0^2 + x_1^2} - r\right)/d_r\right]^2 + (x_2/d)^2 + (x_3/d)^2 \le 1. \tag{6}$$

Empirically selected constants in this expression are $r = 0.94,\ d_r = 0.4,\ d = 0.15$. Figure 1 gives evidence that this is indeed an absorbing domain. For initial points distributed over a border of U we perform numerical solution of the differential equations on an interval T and plot the results in the coordinates

$$R_1 = \left(\sqrt{x_0^2 + x_1^2} - r\right)/d_r,\ \ R_2 = \sqrt{(x_2/d)^2 + (x_3/d)^2}. \tag{7}$$

As the whole figure is placed inside the unit circle $R_1^2 + R_2^2 = 1$, the images of the initial points belong to the interior of U.

In Fig.2 we show a three-dimensional projection to illustrate mutual location of the domains U and $\mathbf{T}(U)$. It is analogous to that considered on the first step of the construction of the Smale – Williams attractor: take a torus ("a plastic doughnut"), stretch it twice, contract transversally, fold twice and squeeze into its original volume. The transformed "doughnut" $\mathbf{T}(U)$ looks like a narrow band because of very strong compression of the phase volume in respective directions in a course of the evolution.

We will verify hyperbolicity conditions required by a theorem (see e.g. [1, 13]) adopted for the problem under consideration. Unlike the general formulation, it is sufficient for us to deal with a diffeomorphism of class C$^\infty$ in the Euclidian space $\mathbb{R}^4$ $\{x_0,\, x_1,\, x_2,\, x_3\}$. That is the Poincaré map $\mathbf{T}(\mathbf{x})$. Evolution of a perturbed state $\mathbf{x} + \delta\mathbf{x}$ corresponds to transformation of the perturbation vector $\delta\mathbf{x}$ in linear approximation $\delta\mathbf{x}' = \mathbf{DT}_\mathbf{x}\delta\mathbf{x}$, where $\mathbf{DT}_\mathbf{x}$ is the Jacobi matrix at $\mathbf{x}$: $\mathbf{DT}_x = \{\partial x_i'/\partial x_j\},\ i, j = 0,\, 1,\, 2,\, 3$. The notion $\mathbf{DT}_\mathbf{x}^{-1}$ designates the derivative matrix for the inverse mapping $\mathbf{T}^{-1}(\mathbf{x})$.

Theorem [1,13]. Suppose that a diffeomorphism $\mathbf{T}$ of class C$^\infty$ maps a bounded domain $U \subset \mathbb{R}^4$ into itself: $\mathbf{T}(U) \subset \operatorname{Int} U$, and $A \subset \operatorname{Int} U$ is an invariant subset for the diffeomorphism. The set A will be uniformly hyperbolic if there exists a constant $\gamma > 1$ and the following conditions hold:

1. For each $\mathbf{x} \in A$ in the space $\mathbb{V}_x$ of 4D vectors $\delta\mathbf{x}$ the expanding and contracting cones $S_\mathbf{x}^\gamma$ and $C_\mathbf{x}^\gamma$ may be defined, such that $\|\mathbf{DT}_\mathbf{x}\mathbf{u}\| > \gamma\,\|\mathbf{u}\|$ for all $\mathbf{u} \in S_\mathbf{x}^\gamma$, and $\left\|\mathbf{DT}_\mathbf{x}^{-1}\mathbf{v}\right\| > \gamma\,\|\mathbf{v}\|$ for all $\mathbf{v} \in C_\mathbf{x}^\gamma$; moreover, for all $\mathbf{x} \in A$ they satisfy $S_\mathbf{x}^\gamma \cap C_\mathbf{x}^\gamma = \emptyset$ and $S_\mathbf{x}^\gamma + C_\mathbf{x}^\gamma = \mathbb{V}_x$.

2. The cones $S_\mathbf{x}^\gamma$ are invariant in respect to action of $\mathbf{DT}$, and $C_\mathbf{x}^\gamma$ are invariant in respect to action of $\mathbf{DT}^{-1}$, i.e. for all $\mathbf{x} \in A$ $\quad \mathbf{DT}_\mathbf{x}(S_\mathbf{x}^\gamma) \subset S_{\mathbf{T}(\mathbf{x})}^\gamma$ and $\mathbf{DT}_\mathbf{x}^{-1}(C_\mathbf{x}^\gamma) \subset C_{\mathbf{T}^{-1}(\mathbf{x})}^\gamma$.

If the formulated conditions are valid for a whole absorbing domain containing the attractor, say, $\mathbf{T}^n(U)$, they are obviously true for the attractor $A = \bigcap_{n=1}^{\infty} \mathbf{T}^n(U)$.

Let us consider in some detail the procedure of computer verification of these conditions. Been given a point $\mathbf{x} = \{x_0,\, x_1,\, x_2,\, x_3\} \in U$, we perform numerical solution of Eqs. (4) on the interval $t \in [0,\ T]$ with the initial state

$$\begin{array}{c} x|_{t=0} = r_0 x_0,\ u|_{t=0} = r_1 x_1 + c_{ux} x, \\ y|_{t=0} = x_2 + c_{yx} x + c_{yu} u,\ v|_{t=0} = x_3 + c_{vx} x + c_{vu} u + c_{vy} y \end{array} \tag{8}$$

and get the image

$$\begin{array}{rl} \mathbf{x}' = \mathbf{T}(\mathbf{x}) & = \{x_0',\, x_1',\, x_2', x_3'\} \\ & = \{x'/r_0,\ (u' - c_{ux} x')/r_1,\ y' - c_{yx} x' - c_{yu} u',\ v - c_{vx} x' - c_{vu} u' - c_{vy} y'\}. \end{array} \tag{9}$$

In parallel, we solve numerically the linearized equations for vectors of small perturbations over the same period. In the original variables they are

$$\begin{array}{ll} \delta\dot{x} = \omega_0 \delta u, & \delta\dot{u} = -\omega_0 \delta x - 2xu\delta x + (A\cos 2\pi t/T - x^2)\delta u + (\varepsilon/\omega_0)\delta y \cos\omega_0 t, \\ \delta\dot{y} = 2\omega_0 \tilde{v}, & \delta\dot{v} = -2\omega_0 \delta y - 2yv\delta y + (-A\cos 2\pi t/T - y^2)\delta v + (\varepsilon/\omega_0) x \delta x. \end{array} \tag{10}$$

Passage to the redefined coordinates and back may be done with the relations

$$\begin{array}{c} \delta x_0 = \delta x/r_0,\ \delta x_1 = (\delta u - c_{ux}\delta x)/r_1,\ \delta x_2 = \delta y - c_{yx}\delta x - c_{yu}\delta u, \\ \delta x_3 = \delta v - c_{vx}\delta x - c_{vu}\delta u - c_{vy}\delta y. \end{array} \tag{11}$$

The equations (10) are solved along the orbit started at $\mathbf{x}$ for four times, each time with such an initial vector $\mathbf{u}$= $\{\delta x_i\}$ that unity is posed in a row from 0 to 3, and other elements are zero. Then, we get four vector-columns and compose a matrix $\mathbf{U} = \mathbf{D}\mathbf{T}_\mathbf{x}$ of them.

Starting at $\mathbf{x}$, an initial perturbation vector $\mathbf{u}$ after one iteration of the Poincaré map yields $\mathbf{u}' = \mathbf{U}\mathbf{u}$. A squared Euclidean norm of this vector is $\|\mathbf{u}'\|^2 = \mathbf{u}^T\mathbf{U}^T\mathbf{U}\mathbf{u}$, where T means the transposition. Using the inverse matrix $\mathbf{U}^{-1}$ we can write as well $\mathbf{u} = \mathbf{U}^{-1}\mathbf{u}'$ and $\|\mathbf{u}\|^2 = \mathbf{u}'^T\mathbf{U}^{-1,T}\mathbf{U}^{-1}\mathbf{u}'$. A condition that $\mathbf{u}'$ represents an image of a vector belonging to the expanding cone $S^\gamma_\mathbf{x}$, is given by an inequality $\|\mathbf{u}'\| > \gamma\|\mathbf{u}\|$, or $\mathbf{u}'^T\left(\mathbf{U}^{-1,T}\mathbf{U}^{-1} - \gamma^{-2}\right)\mathbf{u}' < 0$. Starting at $\mathbf{x}' = \mathbf{T}(\mathbf{x}) = \{x_0',\, x_1',\, x_2', x_3'\}$, an initial vector $\mathbf{u}'$ transforms into $\mathbf{u}'' = \mathbf{U}'\mathbf{u}'$, and we have $\|\mathbf{u}''\|^2 = \mathbf{u}'^T\mathbf{U}'^T\mathbf{U}'\mathbf{u}'$. The expanding cone $S^\gamma_{\mathbf{T}(\mathbf{x})}$ at $\mathbf{x}' = \mathbf{T}(\mathbf{x})$ is determined by an inequality $\|\mathbf{u}''\| > \gamma\|\mathbf{u}'\|$, or $\mathbf{u}'^T\left(\mathbf{U}'^T\mathbf{U}' - \gamma^2\right)\mathbf{u}' > 0$.

The 4×4 matrix $\mathbf{U}'^T\mathbf{U}'$ is positive definite and symmetric. Let $\mathbf{d}_0, \mathbf{d}_1, \mathbf{d}_2, \mathbf{d}_3$ be vectors of the orthonormal basis. The matrix $\mathbf{D} = (\mathbf{d}_0, \mathbf{d}_1, \mathbf{d}_2, \mathbf{d}_3)$ transforms the matrix $\mathbf{U}'^T\mathbf{U}'$ to diagonal form:

$$\mathbf{D}^T\mathbf{U}'^T\mathbf{U}'\mathbf{D} == \{\Lambda_i^2\delta_{ij}\} \tag{12}$$

Let the eigenvalues be enumerated in decreasing order. As we have one expanding and three contracting directions, then, $\Lambda_0^2 > 1$ and $\Lambda_{1,2,3}^2 < 1$. Now, we suppose that γ is selected in such way that $\Lambda_0^2 > \gamma^2$ and $\Lambda_{1,2,3}^2 < \gamma^2$.[2] Then, in the matrix

$$\mathbf{D}^T(\mathbf{U}'^T\mathbf{U}' - \gamma^2)\mathbf{D} = \{(\Lambda_i^2 - \gamma^2)\delta_{ij}\} \tag{13}$$

[2]This property is checked in a course of computations at each analyzed point of the absorbing domain naturally: its violation would entail a non-correct operation of taking a square root of a negative number. The inequalities for eigenvalues of the matrix $\mathbf{U}_\mathbf{x}^T\mathbf{U}_\mathbf{x}$ ensure fulfillment of the condition that a sum of subsets of the linear vector space (that is a set of all possible linear combinations of vectors from the expanding and contracting cones) is the full 4D vector space: $S^\gamma_\mathbf{x} + C^\gamma_\mathbf{x} = \mathbb{V}$.

we have one positive and three negative elements on the diagonal. By an additional scale change along the coordinate axes

$$\mathbf{S} = \{s_i^{-1}\delta_{ij}\},\ s_0 = \sqrt{\Lambda_0^2 - \gamma^2},\ s_{1,2,3} = \sqrt{\gamma^2 - \Lambda_{1,2,3}^2} \tag{14}$$

it is reduced to the canonical form

$$\mathbf{S}^T\mathbf{D}^T(\mathbf{U}'^T\mathbf{U}' - \gamma^2)\mathbf{D}\mathbf{S} = \mathbf{H}' = \{h'_i\delta_{ij}\},\ h'_0 = 1,\ h'_{1,2,3} = -1. \tag{15}$$

A vector $\mathbf{c}$=$\{1,c_1,c_2,c_3\}$ belongs to the expanding cone $S^{\gamma}_{\mathbf{T(x)}}$, if $\mathbf{c}^T\mathbf{H}'\mathbf{c} > 0$, or

$$c_1^2 + c_2^2 + c_3^2 < 1. \tag{16}$$

In the 3D space $\{c_1,c_2,c_3\}$ it corresponds to interior of the unit ball.

With the same transformations, the matrix $\mathbf{U}^{-1,T}\mathbf{U}^{-1} - \gamma^{-2}$ takes a form

$$\mathbf{S}^T\mathbf{D}^T(\mathbf{U}^{-1,T}\mathbf{U}^{-1} - \gamma^{-2})\mathbf{D}\mathbf{S} = \mathbf{H} = \{h_{ij}\}. \tag{17}$$

(Note that it is symmetric: $h_{ij} = h_{ji}$.) A vector $\mathbf{c}$=$\{1,c_1,c_2,c_3\}$ represents an image of a vector belonging to the expanding cone, if $\mathbf{c}^T\mathbf{H}\mathbf{c} < 0$, or

$$\begin{array}{l} h_{00} + h_{01}c_1 + h_{02}c_2 + h_{03}c_3 + h_{10}c_1 + h_{11}c_1^2 + h_{12}c_1c_2 + h_{13}c_1c_3 + \\ h_{20}c_2 + h_{21}c_1c_2 + h_{22}c_2^2 + h_{23}c_2c_3 + h_{30}c_3 + h_{31}c_1c_3 + h_{32}c_2c_3 + h_{33}c_3^2 < 0. \end{array} \tag{18}$$

In the space $\{c_1,c_2,c_3\}$ it corresponds to interior of some ellipsoid. The inclusion $\mathbf{DT_x}(S^{\gamma}_{\mathbf{x}}) \subset S^{\gamma}_{\mathbf{T(x)}}$ means that the ellipsoid has to be placed inside the unit ball. To formulate a sufficient condition for this, we determine a center of the ellipsoid from the equations

$$\begin{array}{l} h_{11}\bar{c}_1 + h_{12}\bar{c}_2 + h_{13}\bar{c}_3 = -h_{10}, \\ h_{21}\bar{c}_1 + h_{22}\bar{c}_2 + h_{23}\bar{c}_3 = -h_{20}, \\ h_{31}\bar{c}_1 + h_{32}\bar{c}_2 + h_{33}\bar{c}_3 = -h_{30}, \end{array} \tag{19}$$

and estimate a distance of this point from the center of the ball:

$$\rho = \sqrt{\bar{c}_1^2 + \bar{c}_2^2 + \bar{c}_3^2}. \tag{20}$$

With a transfer of the origin to the center of the ellipsoid, the equation for its surface becomes

$$h_{11}\tilde{c}_1^2 + h_{12}\tilde{c}_1\tilde{c}_2 + h_{13}\tilde{c}_1\tilde{c}_3 + h_{21}\tilde{c}_1\tilde{c}_2 + h_{22}\tilde{c}_2^2 + h_{23}\tilde{c}_2\tilde{c}_3 + h_{31}\tilde{c}_1\tilde{c}_3 + h_{32}\tilde{c}_2\tilde{c}_3 + h_{33}\tilde{c}_3^2 = R^2, \tag{21}$$

where $\tilde{c}_i = c_i - \bar{c}_i$, and

$$\begin{array}{l} R^2 = -(h_{00} + h_{01}\bar{c}_1 + h_{02}\bar{c}_2 + h_{03}\bar{c}_3 + h_{10}\bar{c}_1 + h_{11}\bar{c}_1^2 + h_{12}\bar{c}_1\bar{c}_2 + h_{13}\bar{c}_1\bar{c}_3 + \\ h_{20}\bar{c}_2 + h_{21}\bar{c}_1\bar{c}_2 + h_{22}\bar{c}_2^2 + h_{23}\bar{c}_2\bar{c}_3 + h_{30}\bar{c}_3 + h_{31}\bar{c}_1\bar{c}_3 + h_{32}\bar{c}_2\bar{c}_3 + h_{33}\bar{c}_3^2). \end{array} \tag{22}$$

Now, we consider a symmetric 3×3 matrix $\mathbf{h} = \{h_{ij}\},\ i,j = 1,2,3$. In the diagonal representation of this matrix, under appropriate orthogonal coordinate transformation $(\tilde{c}_1, \tilde{c}_2, \tilde{c}_3) \to (\xi_1, \xi_2, \xi_3)$, the equation of the ellipsoid surface becomes

$$l_1\xi_1^2 + l_2\xi_2^2 + l_3\xi_3^2 = R^2, \tag{23}$$

where l_1, l_2, l_3 are eigenvalues of $\mathbf{h}$. The largest semiaxis of this ellipsoid is expressed via the minimal eigenvalue:

$$r_{\max} = R/\sqrt{l_{\min}}. \tag{24}$$

A sufficient condition for the ellipsoid to be positioned inside the ball is given by an inequality

$$r_{\max} + \rho < 1. \tag{25}$$

It completes the procedure of verification of the expanding cones inclusion for the point $\mathbf{x}$.

It may be shown that with γ <1 the application of the above procedure in U is equivalent to verification of the condition in the domain $\mathbf{x}\in\mathbf{T}^2(U)$ for contracting cones with the parameter $\gamma' = 1/\gamma > 1$: $\mathbf{DT}_{\mathbf{x}}^{-1}(C_{\mathbf{x}}^{1/\gamma}) \subset C_{\mathbf{T}^{-1}(\mathbf{x})}^{1/\gamma}$. It is so because the cones S^γ and $C^{1/\gamma}$ are complimentary sets: $\bar{S}^\gamma \cup \bar{C}^{1/\gamma} = \mathbb{V}$. (Here S^γ with $\gamma < 1$ corresponds to the cone of vectors, which either expand, or contract, but no stronger than by the factor γ.) Hence, fulfillment of the inequality (25) checked inside U for two parameters γ and $1/\gamma$ would imply that both conditions for expanding and for contracting cones are valid in the domain $\mathbf{T}^2(U)$, which contains the attractor.[3] This is sufficient to draw a conclusion on the hyperbolic nature of the attractor.

The computer verification of the required inclusions for the expanding and contracting cones was performed at the parameter values (2) in the coordinate system (4), (5). Computations of the Poincaré map and of the Jacobi matrices were produced by means of joint numerical solution of the differential equations (1) together with linearized equations (10) on the time interval T. We used the Runge – Kutta method of the 8-th order based on formulas of Dormand and Prince with automatic selection of step (the accuracy for one step was assigned to be 10^{-11}) and an extrapolation method (the accuracy for one step assigned 10^{-15}) [19]. For solution of sets of linear algebraic equations, matrix diagonalization, and eigenvalue problem solving, we used sub-programs from the library LAPACK [20].

In accordance with our computations, at $\gamma^2 = 1.1$ the sufficient condition (25) of correct inclusion for the expanding cones $\mathbf{DT}_{\mathbf{x}}(S_{\mathbf{x}}^\gamma) \subset S_{\mathbf{T}(\mathbf{x})}^\gamma$ is valid in the whole absorbing domain U. To discuss details, let us consider a 3D hypersurface defined by an equation

$$\left[\left(\sqrt{x_0^2 + x_1^2} - r\right)/d_r\right]^2 + (x_2/d)^2 + (x_3/d)^2 = R^2. \tag{26}$$

At $R = 1$ it corresponds to a border of the domain U; at $R < 1$ it belongs to its interior. We can parametrize this hypersurface by three angle coordinates ϕ, ψ, and θ:

$$\begin{aligned} x_0 &= (Rd_r\cos\theta + r)\sin\psi, \quad & x_1 &= (Rd_r\cos\theta + r)\cos\psi, \\ x_2 &= Rd\sin\theta\cos\phi, & x_3 &= Rd\sin\theta\sin\phi. \end{aligned} \tag{27}$$

The variable ψ may be regarded as a phase of the first oscillator at the Poincaré cross-section, and ϕ as a phase of the second oscillator at the same instant. Numerical computations on a 3D grid with step $2\pi/M$ at $M = 50$ show that the value $r_{\max} + \rho = f(R, \phi, \psi, \theta)$ at fixed R depends essentially on ψ and θ, while dependence on ϕ is very weak. On the

[3] At the same γ, the cones S^γ and C^γ have a common border only at $\gamma = 1$, while at $\gamma > 1$ they do not intersect, as required by the theorem conditions: $S_{\mathbf{x}}^\gamma \cap C_{\mathbf{x}}^\gamma = \emptyset$.

plot of the function f one global maximum can be seen of value varied in dependence on ϕ and R. At $R = 1$ and some ϕ the maximum reaches $f_{max} \approx 0.929441$ (that corresponds to a point M on the border of the domain U with coordinates $x_0 = -0.102628$, $x_1 = -0.544957$, $x_2 = 0.000581$, $x_3 = 0.040066$), but remains definitely less than 1, see Fig. 3.[4] Panel (b) illustrates mutual disposition for the cones $\mathbf{DT}_{\mathbf{x}}(S^{\gamma}_{\mathbf{x}})$ and $S^{\gamma}_{\mathbf{T(x)}}$ at the point M. The plot shows a 3D cross-section of the 4D vector space $\mathbb{V}_{\mathbf{T(x)}}$ by a hyperplane orthogonal to the expanding direction. The coordinate axes are principal semiaxes of the ellipsoid representing the cross-section of the cone $S^{\gamma}_{\mathbf{T(x)}}$. Due to scale selection along the axes, it looks like a ball. The ellipsoid representing the cross-section of $\mathbf{DT}_{\mathbf{x}}(S^{\gamma}_{\mathbf{x}})$ looks like a narrow "needle", because of high degree of phase volume compression in two directions. Its disposition inside the large ball testifies the condition $\mathbf{DT}_{\mathbf{x}}(S^{\gamma}_{\mathbf{x}}) \subset S^{\gamma}_{\mathbf{T(x)}}$. The ball circumscribed around the ellipsoid is posed inside the large ball too; that expresses the sufficient condition (25). For smaller R the global maximum of $r_{\max} + \rho$ only decreases (Fig. 4a). Analogous computations with other values of γ indicate that the required inclusions for the cones S take place at least in the interval $0.64 < \gamma^2 < 1.35$ (Fig. 4b). As explained, the correctness of the condition with $\gamma < 1$ implies the condition for the contracting cones $\mathbf{DT}^{-1}_{\mathbf{x}}(C^{1/\gamma}_{\mathbf{x}}) \subset C^{1/\gamma}_{\mathbf{T}^{-1}\mathbf{(x)}}$ in the domain $\mathbf{T}^2(U)$. We conclude that in $\mathbf{T}^2(U)$, both conditions for expanding and contracting cones are true, say, at γ^2=1.1.[5] Hence, the analyzed attractor is uniformly hyperbolic. This assertion, although not proven in a classic mathematical style, follows with definiteness from the theorem, conditions of which have been checked in the computations. Assuming the hyperbolicity established, let us illustrate now some attributes of the hyperbolic dynamics.

To start, we note that dynamics on the attractor is chaotic. In a course of time evolution, both oscillators generate turn-by-turn, passing the excitation one to another. Figure 5 shows typical plots for x and y obtained from numerical solution of Eqs. (1). Panel (a) presents a single sample, and panel (b) shows five superimposed samples of the same signal on successive time intervals. Fig. (b) gives evidence that the process is not periodic. In fact, it is chaos, which manifests itself in irregular displacement of the maxima and minima of the waveforms relative to the envelope on successive time intervals T.

To have a quantitative indicator of chaos we turn to Lyapunov exponents. With multiple iterations of the Poincaré map and Jacobi matrix computations, we trace evolution of four perturbation vectors by means of their subsequent multiplication by the Jacobi matrices obtained in a course of the evolution. At each iteration, the Gram – Schmidt orthogonalization and normalization are performed for the set of vectors. The Lyapunov exponents are determined as the mean rates for growth or decrease of the accumulating sums for logarithms of norms for the vectors (after orthogonalization but before the normalization) [21]. From the computations (10 samples, each of $5 \cdot 10^4$ iterations of the Poincaré map) we obtained the Lyapunov exponents

$$\begin{array}{ll} L_1 = 0.6832 \pm 0.0007, & L_2 = -2.6022 \pm 0.0036, \\ L_3 = -4.6054 \pm 0.0028, & L_4 = -6.5381 \pm 0.0078. \end{array} \qquad (28)$$

[4] For a search of the maximum in a space of three variables at fixed R, we used the Newton method.

[5] Restricting the domain of verification of the condition for expanding cones by the set $\mathbf{T}^2(U)$ one can improve essentially the estimate for maximum allowable γ. In accordance with our computations, the inclusion conditions for expanding and contracting cones inside the domain $\mathbf{T}^2(U)$ are valid yet at $\gamma^2 \approx 1.5$.

Presence of the positive exponent L_1 indicates chaos. (It is close to $\ln 2 = 0.6931$ because of applicability of the approximate Bernoulli map (3).)

Figure 6 shows portraits of the attractor on a plane of variables of the first oscillator. The panel (a) depicts projection of the attractor from the 5D extended phase space on the plane of original variables (x, u). The attractor is shown in gray scales (the darkness reflects a relative duration of residence inside a given pixel). Black dots relate to the Poincaré cross-section, the instants $t_n = nT$. The panel (b) shows the attractor in the Poincaré cross-section on a plane of the redefined coordinates (x_0, x_1) (see (4)). Note an evident visual similarity with the Smale – Williams attractor as depicted in textbooks. The transverse Cantor-like structure is illustrated separately on the panels (c) and (d) by magnified fragments of the previous picture. For quantitative characterization of the fractal structure in the Poincaré cross-section, we have estimated the correlation dimension by means of the algorithm of Grassberger and Procaccia. Using a 4-component time series $\mathbf{x}_n = \mathbf{x}(t_n)$ obtained from numerical iterations of the Poincaré map for n=1÷M, M=40000, we get D=1.2516±0.0018 (as a result of averaging over 10 samples). The dimension estimated from Luapunov exponents with the Kaplan – Yorke formula is $D \approx 1.263$.

From the point of view of theoretical analysis of the hyperbolic attractors, one of the principal features is that intersections of local stable and unstable manifolds if occur must be transversal. In computations, to determine the local manifolds with appropriate accuracy one can use the following scheme. Let us have three points on the attractor obtained one from another by N-fold application of the Poincaré map: $\mathbf{x}_A \to \mathbf{x}_B = \mathbf{T}^N(\mathbf{x}_A) \to \mathbf{x}_C = \mathbf{T}^N(\mathbf{x}_B)$, where N is a sufficiently large integer. To obtain the 1D unstable manifold at B, we consider an ensemble of initial conditions close to A and parametrized by $\Delta\psi$, a small deflection of the angle variable, of order L_1^{-N}: $x_0 = r^A \sin\psi$,, $x_1 = r^A \cos\psi$, $x_2 = x_2^A$, $x_3 = x_3^A$, $r^A = \sqrt{(x_0^A)^2 + (x_1^A)^2}$, $\psi = \psi^A + \Delta\psi$, $\psi^A = \arg(x_1^A + ix_0^A)$. After N iterations of the map $\mathbf{T}$, the points take up positions along the unstable manifold Γ_u^B. To obtain the 3D stable manifold at B we set initial conditions for the Poincaré map close to B: $x_0 = (r^B + \Delta r)\sin\psi_0$, $x_1 = (r^B + \Delta r)\cos\psi_0$, $x_2 = x_2^B + \Delta x_2$, $x_3 = x_3^B + \Delta x_3$, where $r^B = \sqrt{(x_0^B)^2 + (x_1^B)^2}$. Fixing three values ($\Delta r$, Δx_2, Δx_3), which parametrize the manifold, we take as initial guess $\psi_0 = \psi^B = \arg(x_1^B + ix_0^B)$ and perform N iterations of the map. Then, we get a discrepancy $\psi_N - \psi^C$, $\psi_0 = \psi^C = \arg(x_1^C + ix_0^C)$, correct the initial angle variable, $\psi_0' = \psi_0 + \quad (\psi^C - \psi_N)/2^N$, and repeat the procedure, until the error will be less than a given small value.

A graphic representation of the manifolds is not trivial because the phase space is four-dimensional. Let us use a plane of variables (x_0, x_1) relating to the first oscillator. The 1D unstable manifold we show simply as a projection onto this plane. For representation of a three-dimensional stable manifold we will use a curve of intersection of the manifold with a two-dimensional plane $\{x_2 = x_2^B,\ x_3 = x_3^B\}$ projected onto the plane (x_0, x_1). Practically, a sufficient accuracy for coordinates of points on the manifolds is reached, say, at $N \sim 10$. The disposition of the local manifolds revealed from the computations is illustrated in Fig. 7. The invariant set that consists of the unstable manifolds coincides with the attractor itself. It is enclosed in the toroidal absorbing domain going turn by turn around "the hole of the doughnut". On the other hand, the local stable manifolds are posed across the "tube" that forms a surface of the toroid. In the two-dimensional diagram the stable manifolds look like "speaks of a wheel". Due to such mutual location,

the stable and unstable manifolds can intersect only transversally, and no tangencies do occur.

As stated in this article, in the four-dimensional phase space of Poincaré map for the system of two non-autonomous coupled van der Pol oscillators there exists a toroidal absorbing domain, containing a uniformly hyperbolic attractor. This conclusion is based on computer verification of conditions formulated in terms of appropriate inclusion of expanding and contracting cones defined in the tangent vector spaces associated with the points of the absorbing domain. Hence, our model delivers a long-time expected example of a simple physically realistic system with hyperbolic attractor. With this example, it will be possible to construct other models with hyperbolic chaos, exploiting structural stability intrinsic to the hyperbolic attractors. In fact, a physical experiment demonstrating attractor of this type has been performed already on a basis of coupled electronic oscillators [16]. In applications, the systems with hyperbolic chaos may be of special interest because of their robustness (structural stability). An interesting, and now a substantial direction is constructing chains, lattices, networks on a base of elements with hyperbolic chaos [22]. Models of this class may be of interest for understanding deep and fundamental questions, like the problem of turbulence.

This research was supported by RFBR grant No 06-02-16619.

References

[1] Ya.G. Sinai, in: Nonlinear Waves. Ed. A.V. Gaponov – Grekhov (Nauka Moscow 1979) 192 (in Russian).

[2] J.-P. Eckmann and D. Ruelle, Rev. Mod. Phys. **57** (1985) 617.

[3] R.L. Devaney, An Introduction to Chaotic Dynamical Systems (Addison-Wesley, New York, 1989).

[4] L. Shilnikov, Int. J. of Bifurcation and Chaos **7** (1997) 1353-2001.

[5] A. Katok and B. Hasselblatt, Introduction to the Modern Theory of Dynamical Systems. (Cambridge: Cambridge University Press, 1995).

[6] V. Afraimovich and S.-B. Hsu, Lectures on chaotic dynamical systems, AMS/IP Studies in Advanced Mathematics, **28**, American Mathematical Society, Providence, RI; International Press, Somerville, MA (2003).

[7] E. Ott, Chaos in Dynamical Systems (Cambridge University Press, 1993).

[8] V.S. Anishchenko, V.V. Astakhov, A.B. Neiman, T.E. Vadivasova, and L. Schimansky-Geier, Nonlinear Dynamics of Chaotic and Stochastic Systems. Tutorial and Modern Development (Springer, Berlin, Heidelberg, 2002).

[9] V.S. Afraimovich, V.V. Bykov, and L.P. Shil'nikov, Sov. Phys. Dokl. **22** (1977) 253.

[10] K. Mischaikow and M. Mrozek, Bull. Am. Math. Soc. **32** (1995) 66.

[11] L.P. Shil'nikov and D.V. Turaev, Doklady RAS **342** (1995) 596 (in Russian).

[12] T.J. Hunt and R.S. MacKay, Nonlinearity **16** (2003) 1499.

[13] T.J. Hunt, PhD Thesis, Univ. of Cambridge (2000).

[14] V. Belykh, I. Belykh and E. Mosekilde, Int. J. of Bifurcation and Chaos **15** (2005) 3567.

[15] S.P. Kuznetsov, Phys. Rev. Lett. **95** (2005) 144101.

[16] S.P. Kuznetsov and E.P. Seleznev, JETP **102** (2006) 355.

[17] V.I. Arnol'd, Ordinary Differential Equations (Springer-Verlag, Berlin,1992).

[18] A.A. Andronov, A.A. Vitt, S.E. Khaikin, Theory of Oscillators (Dover Publications, New York, 1966).

[19] E. Hairer, S.P. Nørsett, and G. Wanner, Solving Ordinary Differential Equations I. (Springer Verlag, 1993).

[20] LAPACK, version 3.0: http://www.netlib.org/lapack (2000).

[21] G. Benettin, L. Galgani, A. Giorgilli, J.-M. Strelcyn, Meccanica, **15** (1980) 9.

[22] L.A. Bunimovich and Ya.G. Sinai, Nonlinearity, **1** (1988) 491.

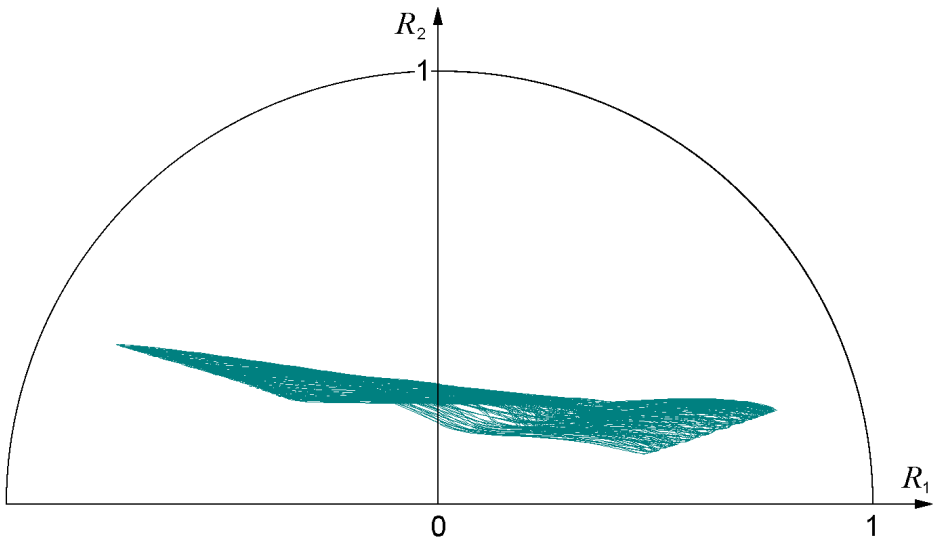

Figure 1: Graphical evidence that the domain U defined by (6) is absorbing. For initial points distributed over a border of U, the resulting data from numerical solution of the differential equations over a period T plotted in coordinates (7) fit inside the unit circle $R_1^2 + R_2^2 = 1$.

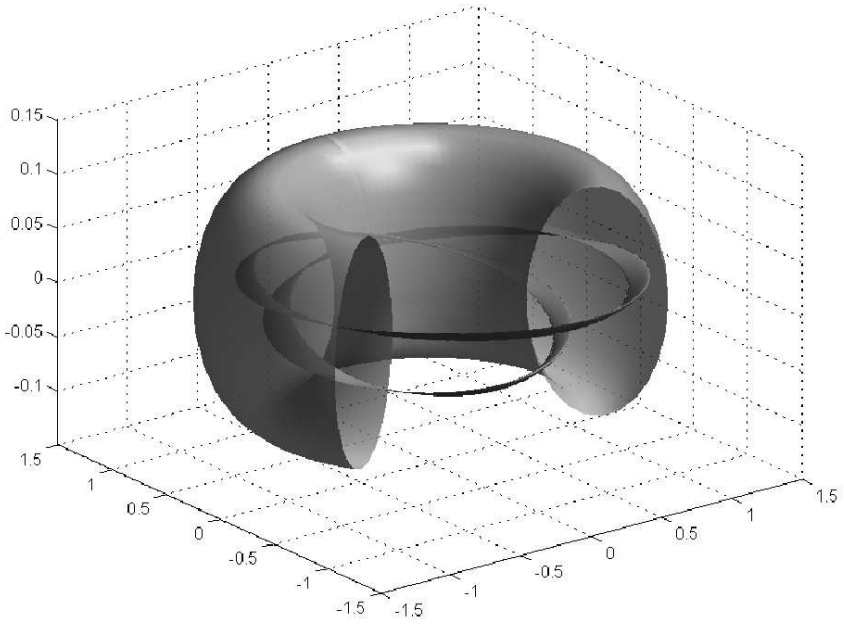

Figure 2: The toroidal absorbing domain U and its image $\mathbf{T}(U)$ shown in a 3D projection. Variables x_0, x_1 are plotted along the axes in the horizontal plane, and x_2 along the vertical axis. The fourth variable x_3 corresponds to direction of the projecting.

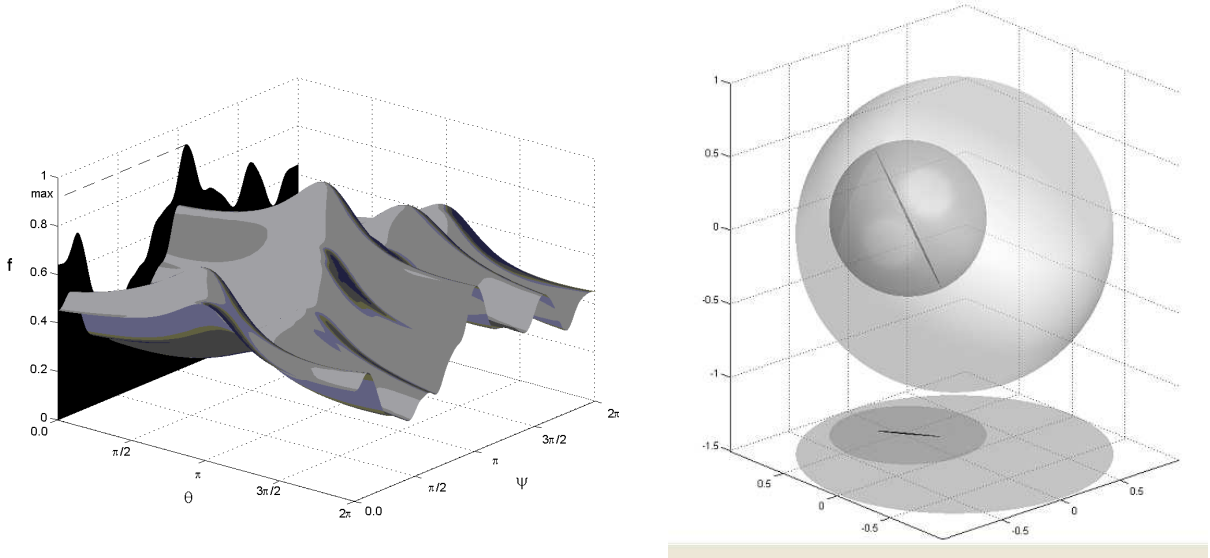

(a) (b)

Figure 3: A plot of the function $r_{\max} + \rho = f(R, \phi, \psi, \theta)$ at $R = 1$ and $\phi = 1.25665$ (a) and a diagram illustrating mutual disposition of the 3D cross-sections of the cones $\mathbf{DT}_{\mathbf{x}}(S^{\gamma}_{\mathbf{x}})$ and $S^{\gamma}_{\mathbf{T(x)}}$ at the point of global maximum of $r_{\max} + \rho$.

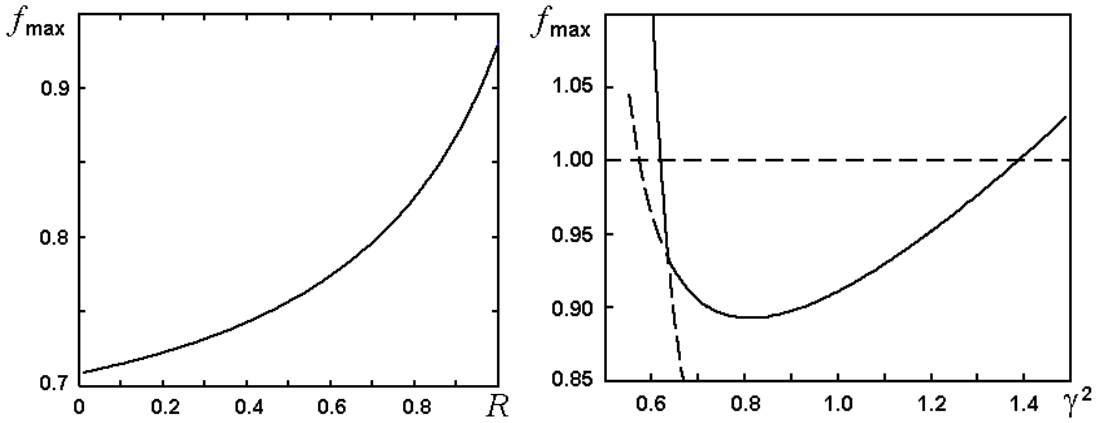

Figure 4: Value of the global maximum of the function $f = r_{\max} + \rho$ on a hypersurface (26) versus parameter R (a) and the global maximum value over the whole absorbing domain U in dependence on parameter γ.

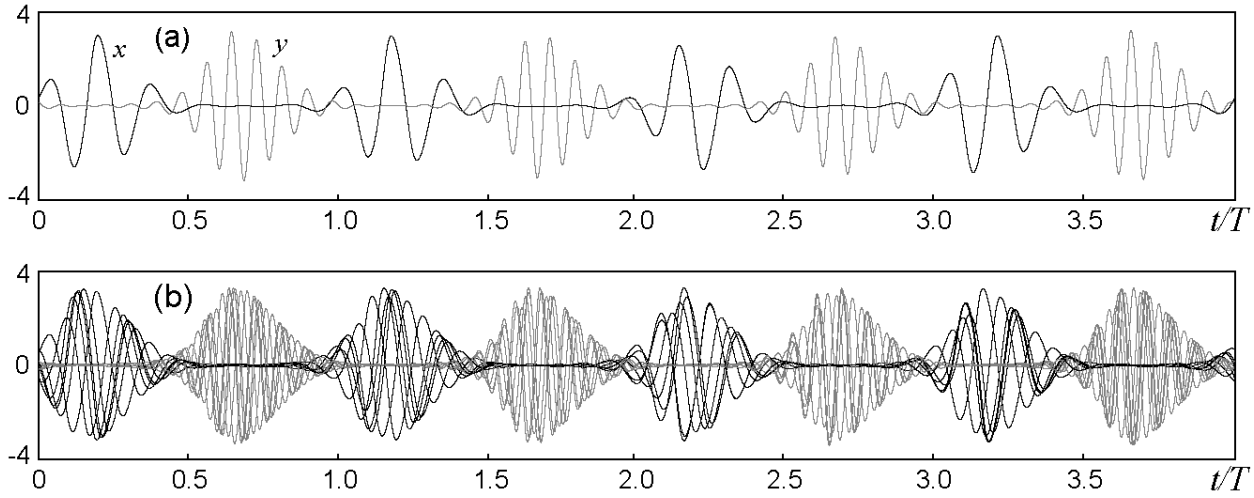

Figure 5: Typical patterns of time dependences for the variables x and y obtained from numerical solution of Eqs. (1) at $T = 6$, $A = 5$, $\varepsilon = 0.5$. Panel (a) presents a single sample, and panel (b) shows five superimposed samples of the same signal on successive time intervals.

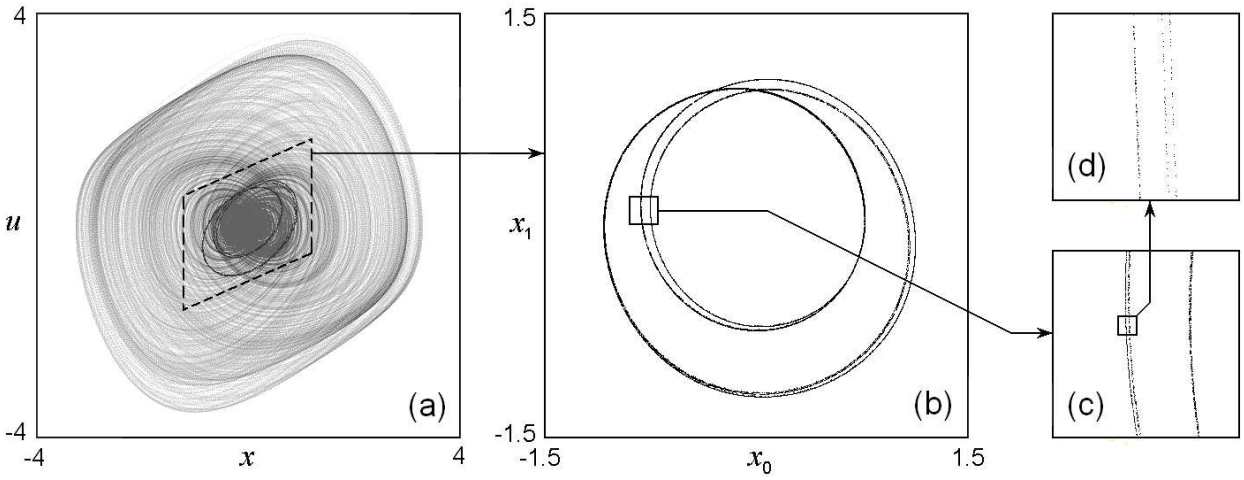

Figure 6: Portraits of the attractor on a plane of variables of the first oscillator: (a) – projection of the attractor from the 5D extended phase space on the plane of original variables (x, u); (b) – the attractor in the Poincaré cross-section on a plane of the redefined coordinates (4); (c), (d) – details of the Cantor-like transverse structure.

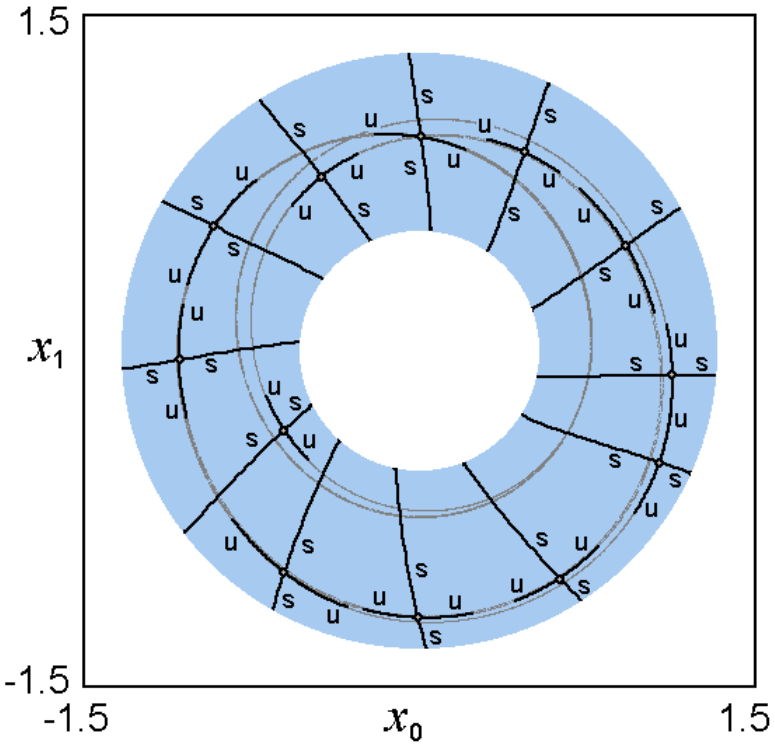

Figure 7: A diagram on the plane of variables (x_0, x_1) illustrating mutual location of local unstable (u) and stable (s) manifolds for a set of points on the attractor in the Poincare cross-section. The gray ring-shaped area depicts a projection of the absorbing domain U.